Bull. Min. Res. Exp. (2024) 174: 37-53

Bulletin of the Mineral Research and Exploration

http://bulletin.mta.gov.tr

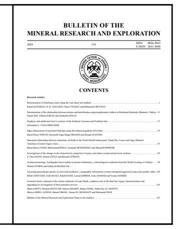

Porphyry and epithermal Au-Cu systems of the Southern Caucasus and Northern Iran

Alexander G. TVALCHRELIDZE[a*]

[a] *Institute of Mineral Resources, Tbilisi State University, 11 Mindeli Str., 0186 Tbilisi, Georgia*

Research Article

Keywords:
Epithermal, Porphyry, Gold, Copper, Paleothermal Field.

ABSTRACT

This article presents tangible geological evidence for the coexistence of porphyry copper and epithermal gold systems within single polygenic deposits and provides a paleothermophysical model for their origins. A brief metallogenic analysis of the Southern Caucasus and Northern Iran has shown that such deposits are confined to long-living calc-alkaline island arcs and were formed during their orogenesis. Examples of complex Sonajil (Iran), Gharta, and Merisi (Georgia) deposits are considered. The investigation has shown that for combined porphyry and epithermal ore formation, some preconditions are suggested to exist: (i) a source of anomalous energy that exceeds the thermodynamics of the enclosing environment; (ii) the existence of a temperature gradient that determines conventional flows of fluids composed of endogenous and meteoric constituents (proven by rhythmical zoning of ore lodes); (iii) the stability of such conditions for a period of sulfide ore formation. However, such a process of sulfide ore formation cannot explain the formation of high sulfidation gold deposits. The precipitation of native gold requires phreatic collapse in the ore conduit channel, already after the formation of hydrothermally altered rocks, and this event results in the creation of either hydrothermal breccias often with jigsaw-fit texture or brecciated vuggy silica where host rocks and hydrothermally altered rocks are cemented by a gold-bearing quartz matrix.

Received Date: 24.04.2023
Accepted Date: 21.11.2023

1. Introduction

By the end of the recent and the beginning of the new centuries, our understanding of the metallogenic setting and genesis of gold, copper, and polymetallic mineralization in the Southern Caucasus and Northern Iran, as well as of the entire Tethys Belt, has dramatically changed. Previously, they were thought to represent perhaps simultaneous but separate products of different ore-forming processes. Today, however, they are considered as deposits united by a common origin and separated from their original magmatic sources by varying distances. For instance, gold and base metal deposits in the Southern Caucasus were traditionally classified into three main types: Volcanogenic gold and base metal massive sulfides of the Kuroko type, hydrothermal gold and polymetallic vein deposits, and porphyry copper (with or without gold) stockwork veins (Tvalchrelidze, 1980 and 1984). This approach significantly limited the possibilities for new discoveries, as exploration was based on incorrect assumptions. As a result, the resource base of the regional stakeholder countries began to deplete. For example, at the beginning of the new millennium, Türkiye gold resource base was considered to be extremely limited, and the prospects for new discoveries were viewed pessimistically (Engin, 2003).

Identification of low, intermediate, and high sulfidation epithermal gold deposits, investigation of

Citation Info: Alexander, G. T., 2024. Porphyry and epithermal Au-Cu systems of the Southern Caucasus and Northern Iran. Bulletin of the Mineral Research and Exploration 174, 37-53. https://doi.org/10.19111/bulletinofmre.1394073

*Corresponding author: Alexander G. TVALCHRELIDZE, sandrotval@gmail.com

their typomorphic features, and the development of a comprehensive methodology for their prospecting and exploration (Arribas, 1995; Hedenquist, 2000; Goldfarb et al., 2001; Payot et al., 2005; John et al., 2018; Wang et al., 2019) led to fast discoveries of new gold deposits in Türkiye (Oyman et al., 2003; Diarra et al., 2019; Aluç et al., 2020; Gülyüz et al., 2020), the Lesser Caucasus (Bogdanov et al., 2013; Moritz et al., 2017; Veliyev et al., 2018; Imamverdiyev et al., 2021), and Iran (Mehrabi et al., 2008; 2014; Aghazadeh et al., 2015; Heidari et al., 2015; Sholeh et al., 2016). These discoveries were extremely important for improving the resource base of the corresponding countries, which is vital for their economic development (Tvalchrelidze, 2003). Correspondingly, the current state of mining, for instance in Türkiye, has significantly improved (Ersoy, 2022; Hastorun, 2022).

New metallogenic models have proven that both epithermal and porphyry deposits are related to the development of calc-alkaline island arcs during subduction and orogenic stages (Yigit, 2006; 2009; Mederer et al., 2013; Moritz et al., 2016). Therefore, porphyry and epithermal deposits are traditionally described separately, without paying any attention to a possible genetic relation between them (Ghaderi et al., 2018; Kuşcu et al., 2019). Even the models for these types of mineralization are generated separately (Sinclair, 2007; Taylor, 2007; Berger et al., 2008; John, 2010; John et al., 2018). Commonly, these models are based on typomorphic features of world-scale classical mines (see, for instance, Boomeri et al., 2010). However, already in 2000, R.H. Sillitoe outlined a genetic unity of porphyry copper and epithermal gold mineralization (Sillitoe, 2000). During the following years, a lot of evidence of gold presence in porphyry copper deposits was released (Shafiei and Shahabpour, 2008; Hajalilou and Aghazadeh, 2016). Nonetheless, descriptions of real natural examples of telescoping and superposition of porphyry, low, intermediate, and high sulfidation epithermal systems are extremely rare, and I found no comprehensive numeric models of such systems. That is why in this article, I will both present tangible geological evidence for the coexistence of such systems and attempt to provide a corresponding paleothermophysical model for their genesis.

2. Metallogenic Setting of Epithermal and Porphyry Systems

2.1. The Southern Caucasus

The distribution of epithermal gold and porphyry copper (± gold) systems in the Caucasus, as shown in Figure 1, reveals that the deposits are uniquely positioned within the Lesser Caucasus and confined to two tectonic zones. The first is the Late Cenozoic rift zone (known as the Adjara-Trialeti zone), which extends beyond Georgia into Türkiye (Adamia et al., 2011). Originating in the Late Alpine (Paleogene-Neogene) period atop the Cretaceous cover of the Transcaucasian Microplate, today it is overlaid by the intermountain trough (Adamia et al., 1981). Within this zone, Neogene homodrome basalt-andesite-rhyolite volcanism expands from the rift's eastern edge (where tuffaceous sandstones and clays form a rhythmical series) towards the west (where typical basaltic and then andesitic volcanic flows are succeeded by rhyiodacitic and rhyolitic volcanic cones interspersed with tuffites). Alkalinity gradually increases in the same direction. In the Late Neogene, several quartz diorite to quartz monzonite massifs were intruded, predominantly in the rift's central and western, more tectonically active parts. Orogenesis here concluded by the end of the Neogene, just before the Quaternary period. The described volcanic-plutonic affinity is marked by several typomorphic deposits, displaying signs of porphyry copper ores in conjunction with either high sulfidation gold mineralization or intermediate sulfidation gold-polymetallic lodes. These types of mineralization will be briefly described below.

The second zone — the Middle Jurassic-Cretaceous Island arc — is identified as the Somkhito-Karabakh zone of global extent (Tvalchrelidze, 1980; 1984). This volcanic belt spans territories of Armenia, Azerbaijan, Georgia (where it is covered by Cenozoic, Early Quaternary, andesite-basaltic nappes), and then extends to Türkiye and beyond. The modern metallogenic model of this zone has been elaborated by an international team of Swiss, Georgian, Armenian, and Azeri geologists (Mederer et al., 2013; Richards, 2015; Moritz et al., 2016; 2017).

In both zones, two volcanic-plutonic ore-bearing affinities have developed. The Middle Jurassic

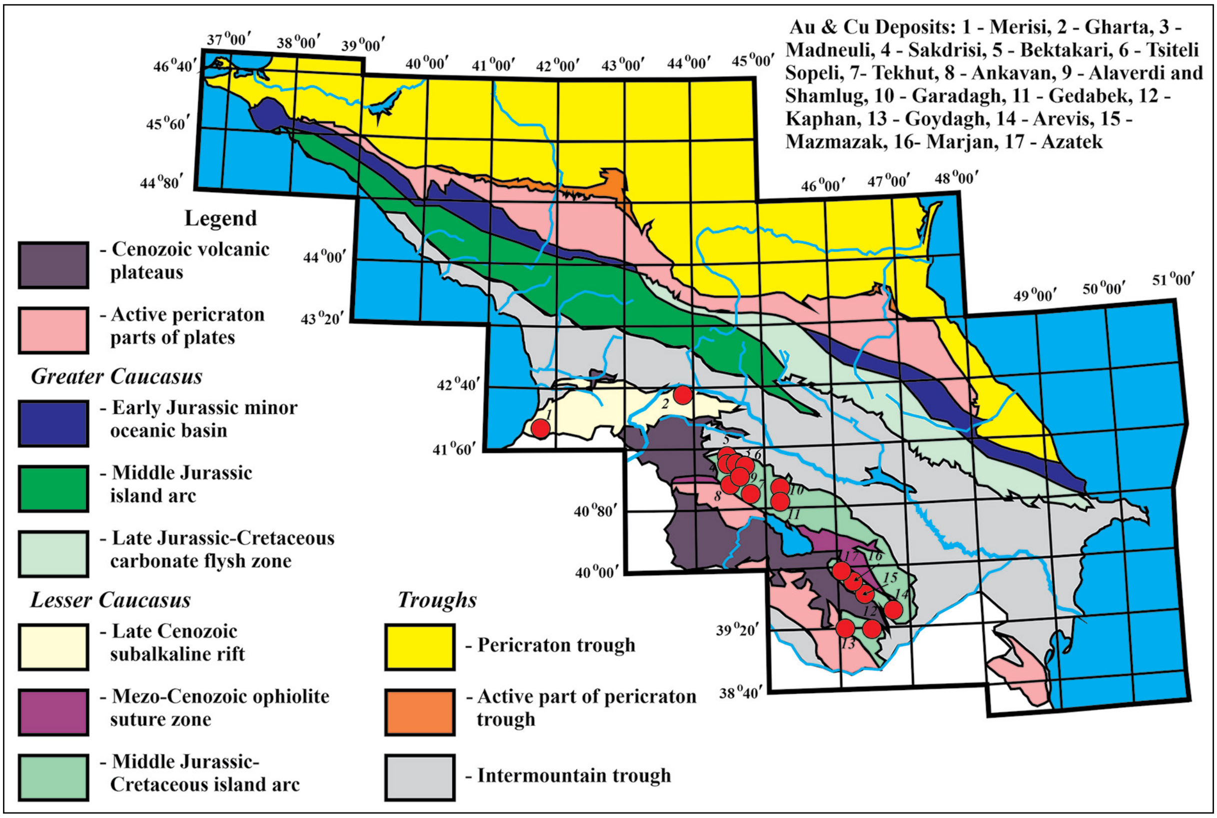

Figure 1- Distribution of the most important porphyry copper (± gold) and high, intermediate, and low sulfidation gold deposits of the Caucasus. Map of metallogenic zoning is modified from Adamia et al. (2011) by author.

rocks, lying directly upon the crystalline basement of the Transcaucasian Microplate, start with a basal conglomerate that overlaps Paleozoic granites. In Armenia and Azerbaijan, a thick calk-alkaline subaqueous andesitic volcanic-sedimentary series has developed. However, north-westward towards Georgia, this island arc affinity decreases in thickness, and Middle Jurassic volcanic rock outcrops become rare. During Bathonian times, this affinity was intruded by vast quartz diorite bodies, one of which, the Shnokh-Kokhp massif, controls the world-class Tekhut Au-Cu porphyry mine (no. 7 in Figure 1) with ore reserves of 460 million tons and copper grade of 0.35% (Marutani, 2003). Cretaceous sediments in Armenia and Azerbaijan are represented only by limestones with insignificant thickness.

Conversely, in Georgia, the thickness of Cretaceous rocks sharply increases, hosting rich ore-bearing Cretaceous andesitic (minor basalt-andesite-dacite-rhyolite) calk-alkaline formation which formed numerous central-type volcanoes and vast fields of acid subaqual pyroclastics in intervocalic areas. This sequence is especially thick (up to 1-1.5 km) within the Bolnisi Mining District, which hosts the great majority of the country's gold and copper reserves (no 3-6 on Figure 1). The sequence is intruded by several quartz diorite bodies the significance of which in ore formation is discussed below.

Among the deposits of the Bolnisi Mining District, the largest one is Madneuli intermediate sulfidation mine with primary ore reserves of 93.1 million tons and metal inventories in them: copper – 542 thousand tons; zinc – 79.8 thousand tons; lead – 8.2 thousand tons; silver – 134 tons; gold – 53.8 tons (Tvalchrelidze, 2003). The mine is the main copper and gold producer in Georgia.

Petrology of both Middle Jurassic and Cretaceous volcanic-plutonic affinities was described in detail some 35 years ago (Tvalchrelidze, 1987).

2.2. Northern Iran

Figure 2 analyses the distribution of typomorphic porphyry copper (± gold) and primarily high

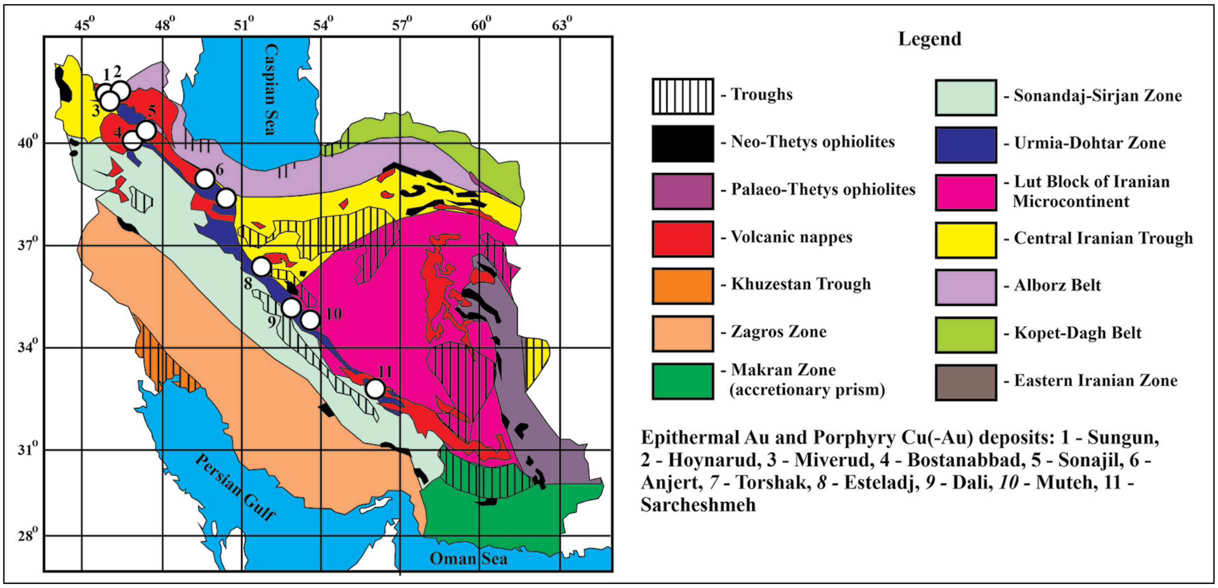

Figure 2- Distribution of typomorphic porphyry Cu (± Au) and epithermal gold deposits of Iran. Map of metallogenic zoning is drawn from Kaviani et al. (2009) modified by author.

sulfidation gold deposits of Iran. These deposits include world-class mines such as Sungun (no. 1 on Figure 2) with recoverable ore reserves of 861 million tons and copper grade of 0.6% (Hosseini et al., 2017) and Sarcheshmeh (no. 11 on Figure 2) with ore reserves of 1538 million tons and a copper grade of 0.58% (Boomeri et al., 2010).

It is evident from Figure 2 that all typomorphic deposits, without exception, are associated with the Urmia-Dokhtar metallogenic zone. This zone represents an andesitic island arc that underwent orogenesis in the Late Neogene – Early Quaternary period. During the 1980s, the extensive development of orogenic magmatism, with still active volcanoes like Sakhand and Sabalan, was not fully understood (Berberian and King, 1981), but it is now clear that this zone continues to be subject to ongoing subduction beneath the Iranian Microcontinent (Kaviani et al., 2009).

In Northern Iran, the Urmia-Dokhtar zone is overlapped by Early Quaternary basaltic nappes and borders the Alborz magmatic belt to the north and the Sanandaj-Sirjan metamorphic zone to the southwest. The latter represented a rift zone that had undergone orogenesis and metamorphism before the Alpine period (Kaviani et al., 2009; Richards, 2015).

Thus, both in the Southern Caucasus and Northern Iran, porphyry copper-gold as well as epithermal ore-forming systems are related to long-lived island arcs that have experienced relatively continuous subduction followed by active development of orogenic magmatism. As a rule, these systems form individual porphyry, high, intermediate, and low sulfidation deposits, but seldom do deposits bear features of different mineralization types. Below, such examples are considered.

3. Combination of Ore-Forming Systems

3.1. Porphyry and High Sulfidation Systems – Sonajil Deposit, Northern Iran

The Sonajil Deposit is located in the East Azerbaijan Province of Iran, near Heris city, approximately 85 km from Tabriz, the province capital. The deposit has been extensively explored by our international team. To date, recoverable reserves of high sulfidation gold ores have been estimated, and gold-producing open pit mines, a heap, and a Carbon-in-Leach (CIL) plant are under construction. The estimated total resources of the gold-bearing site are 7.6 million tons with gold grade of 1.5 g/t, hosting approximately 361 thousand troy ounces of the metal. Porphyry copper ores are currently under extensive exploration. All 12 drilled boreholes have intersected porphyry ores with an average copper grade of 0.4%. The explored vertical interval of mineralization now exceeds 600 m. In these boreholes, the first indications of gold presence with commercial grades were identified.

Figure 3 presents the model geological map of the Sonajil deposit. The geological structure of the deposit is complex. The geological section begins with an Eocene volcanic suite of basalt-andesitic composition, which consists of basalt and andesite lavas, volcanic breccias of the same composition, tuffs, and tuffaceous volcanic-sedimentary rocks. In the ascending sequence, this suite is replaced by Miocene sandstones and marls. The overall sequence concludes with an Early Quaternary volcanic flow of basalt and dolerite composition, which occupies the highest hypsometric level of the terrain.

The Eocene volcanic sequence is intruded by two stages of an igneous complex. Outcrops of two phases of the Inchekh intrusive body are observed in the central part of the area. The first phase is composed of alkali rocks – monzonites and syenites, whereas the second phase consists of calc-alkaline quartz monzonites and microdiorites. These rocks exhibit porphyritic structures and can be interpreted as a root part of a volcano. The younger Sonajil intrusive stage has a well-expressed hypabyssal character and is represented by mica granites and monzonites.

The deposit comprises two sites. The epithermal high sulfidation gold mineralization site is situated 4.5 km southwestward from the porphyry copper deposit. The ore-bearing structure of this deposit trends northwestward (azimuth 320-340°), with a length of about 1400 m, a width from 10 to 50 m, and an incidence angle of 45-60° to the west-south-west. Ore mineralization is traced up to a depth of 200 m from the surface. Within this deposit, the gold-bearing body is presented by hydrothermal breccia, where fragments of hydrothermally altered (quartz + sericite) andesites are cemented by grey quartz. The quartz matrix of the breccias, occasionally accompanied by calcite, is remarkably thick (more than 200 m) from the surface. The breccia exhibits a jigsaw-fit texture, the origin of which has been detailed in several publications (Figure 4a, Cas et al., 2011).

Porphyry copper deposit, situated in the north-eastern part of the deposit, is presented by typical medium-grade ores in hydrothermally altered (quartz + enargite) intrusive rocks, mainly diorites of both Inchekh and Sonajil intrusive bodies (Figure 4b). The orebody is under extensive drilling campaign because prospects to discover a world class copper-gold deposit are very high.

Thus, the key features of the deposit important for further discussion are as follows:

1. Porphyry and high sulfidation epithermal sites are spatially separated.

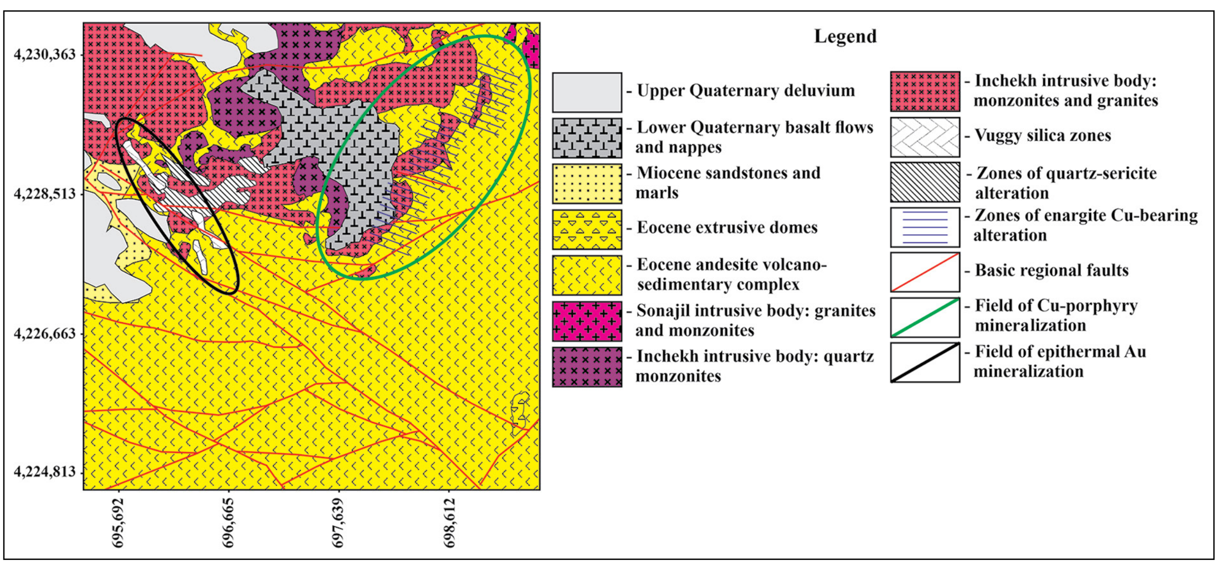

Figure 3- Model geological map of Sonajil deposit, This study.

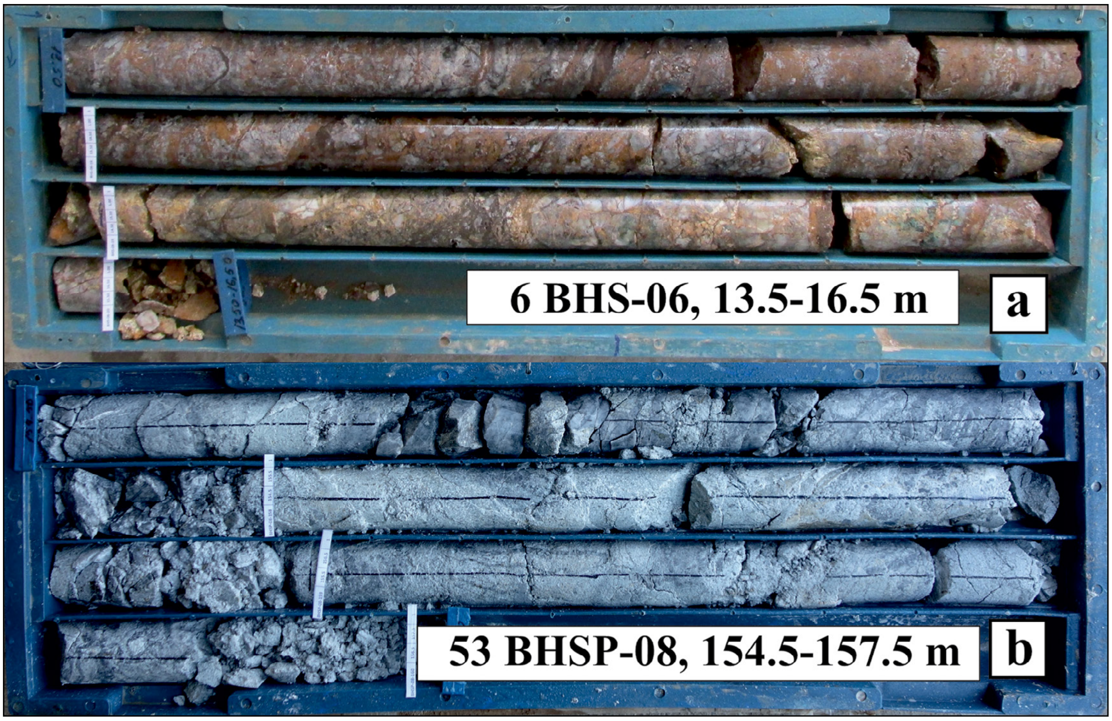

Figure 4- Typical ores of Sonajil deposit, a) gold ores presented by thin impregnation of free gold in the hydrothermal breccia with jigsaw-fit texture; debris of hydrothermally altered quartz-sericite rocks are cemented by quartz. Average Au grade of the interval is 1.41 g/t. b) porphyry gold-copper ores in hydrothermally altered diorites. Average grades of the interval: Copper – 0.56%, gold – 0.74 g/t.

2. Gold mineralization occurs in hydrothermal breccia, formed later than the country andesitic rocks were hydrothermally altered.

3.2. Vertical Zoning of Epithermal High Sulfidation and Porphyry Systems – Gharta Deposit, Georgia

The Gharta deposit is located in the Kareli District, Shida Kartli Region of Georgia, approximately 152.5 kilometers from Tbilisi, the capital city, at the northern slope of the Trialeti Ridge in the Lesser Caucasus. Metallogenically, it is situated at the north-eastern edge of the Adjara-Trialeti rift zone (Figure 1). The deposit has been the subject of extensive exploration by our international team. To date, having covered only about 15% of the deposit's area with a drilling campaign, we have already identified 9.1 million tons of high sulfidation gold with an average gold grade of 0.93 g/t and 62.8 million tons of porphyry copper ores with an average copper grade of 0.42%. A model geological map of the deposit is represented in Figure 5.

The geological structure of the deposit features an area covered by outcrops of Late Neogene intrusive body of quartz diorite composition, which has intruded into Paleogene-Lower Neogene rhythmical slates, argillites, and aleurolites, as well as Upper Cretaceous chemogenic limestones. The host rocks are mainly preserved as relics within the intrusive body and are only visible in the north-western part where the intrusive contact with the mentioned rhythmical slate suite is observed. Numerous mainly sub-latitudinal faults with steep, subvertical dips are present. The entire structure, including the ore zone, is inclined to the east at an angle of 35-45°.

The ore zone has an irregular ellipsoid shape and is presented by hydrothermally altered rocks developed exclusively within the intrusive rocks. Two contrasting types of metasomatic alterations were identified. Within the epithermal gold bonanza zones developed at upper horizons in the western flank of the mineralized zone, hydrothermally brecciated and often fractured vuggy silica is observed (Figure 6a), where debris of quartz diorite and early products of its hydrothermal alteration – quartz-sericite rocks are cemented by grey quartz. At deeper horizons, porphyry copper ores are

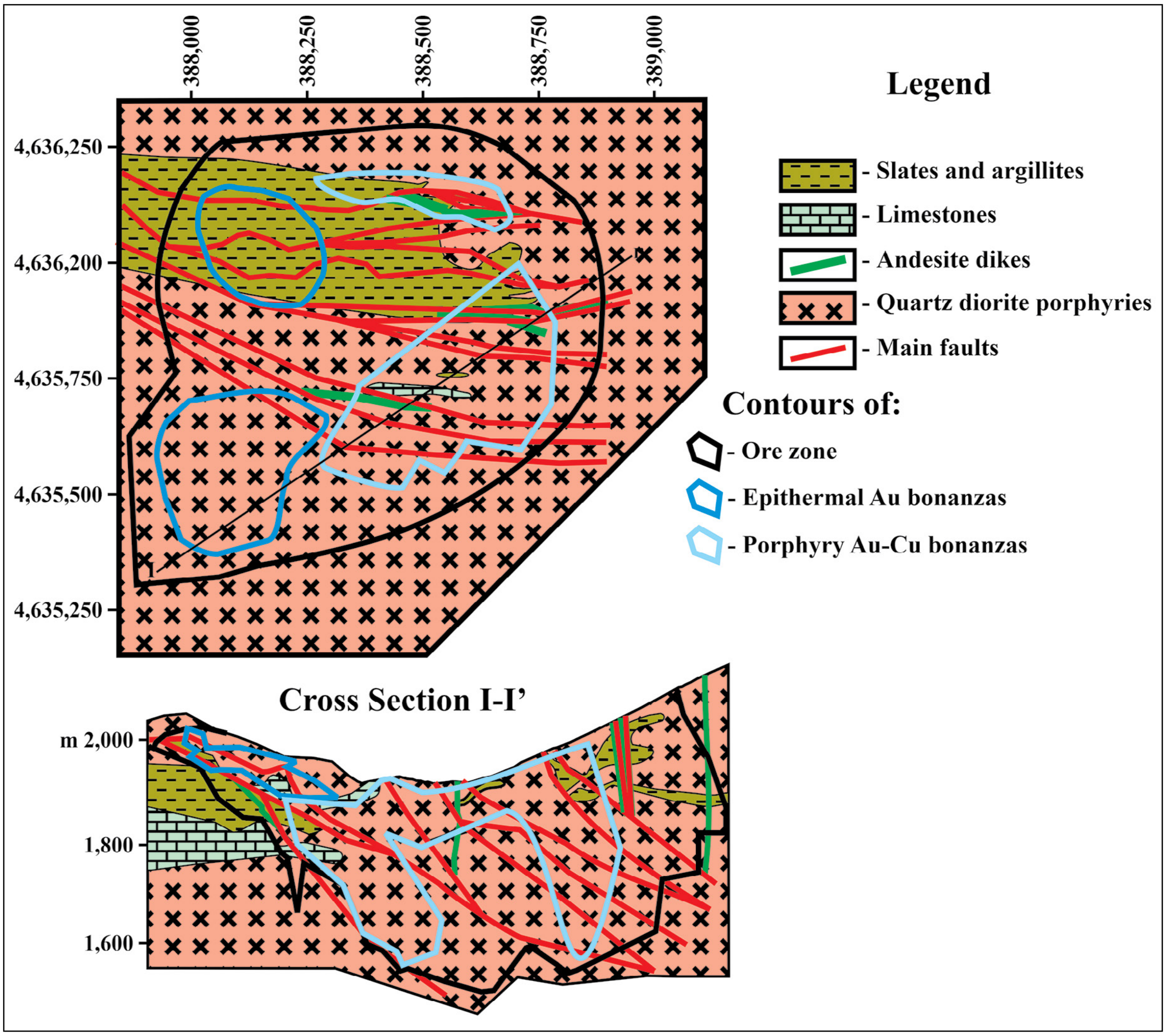

Figure 5- Model geological map of Gharta deposit. This study.

hosted by high-temperature quartz-sericite-garnet-bearing rocks with intense development of epidote. Development of garnet (andradite, as identified diffractometrically) is sometimes so pronounced that quartz diorites are altered to a monomineralic "garnetite" (Figure 6b).

A well-pronounced vertical zoning is characteristic of the deposit (Figure 7). At upper horizons, epithermal high sulfidation gold ores are developed. Beneath 100 meters from the surface, ores are enriched by chalcopyrite, which sometimes creates high-grade ores (Borehole BHG-03 on Figure 7). At deeper horizons, gold-free porphyry copper ores are present. It is crucial to note for further discussion that an ore-free space always exists between gold and copper ores, although this interval is hydrothermally altered in the same manner and with the same intensity as in ore bonanza zones.

3.3. Intermediate Sulfidation and Porphyry Copper Systems – Merisi Mining District, Georgia

The Merisi mining district, identified as no. 1 on Figure 1, is situated in Mount Adjara, approximately 60 km from Batumi, the capital of the Adjara Autonomous Republic of Georgia, and is positioned right on the state border with Türkiye. The district was extensively explored in the 1930s to 1960s, and copper mining was conducted even during the First World War. Currently, only vein-type intermediate sulfidation gold-bearing small deposits have been thoroughly explored, but the primary prospects of the district are related to the porphyry copper system and

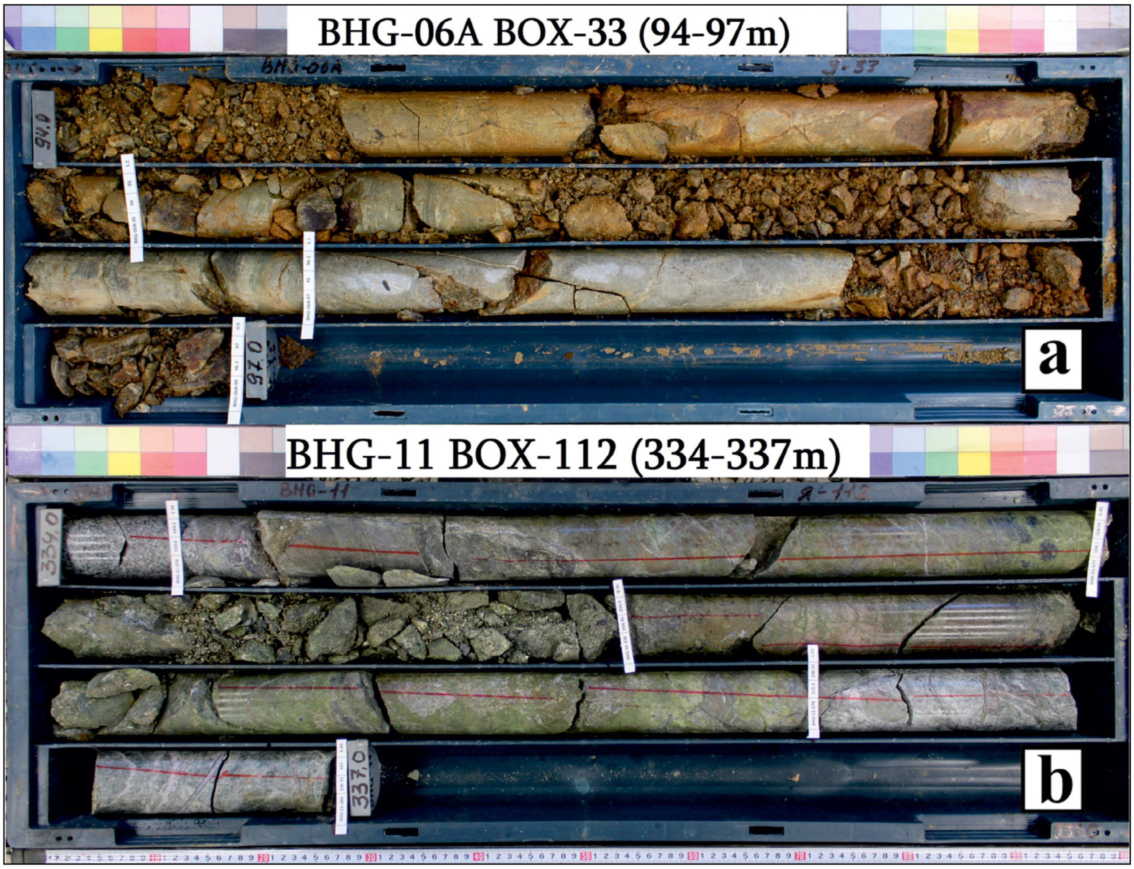

Figure 6- Typical epithermal high sulfidation gold and porphyry copper ores, a) brecciated and fractured vuggy silica; average gold grade of the interval – 3.70 g/t, b) quartz-sericite-garnet (andradite) rock with epidote (green) nests; average copper grade of the interval – 1.38%.

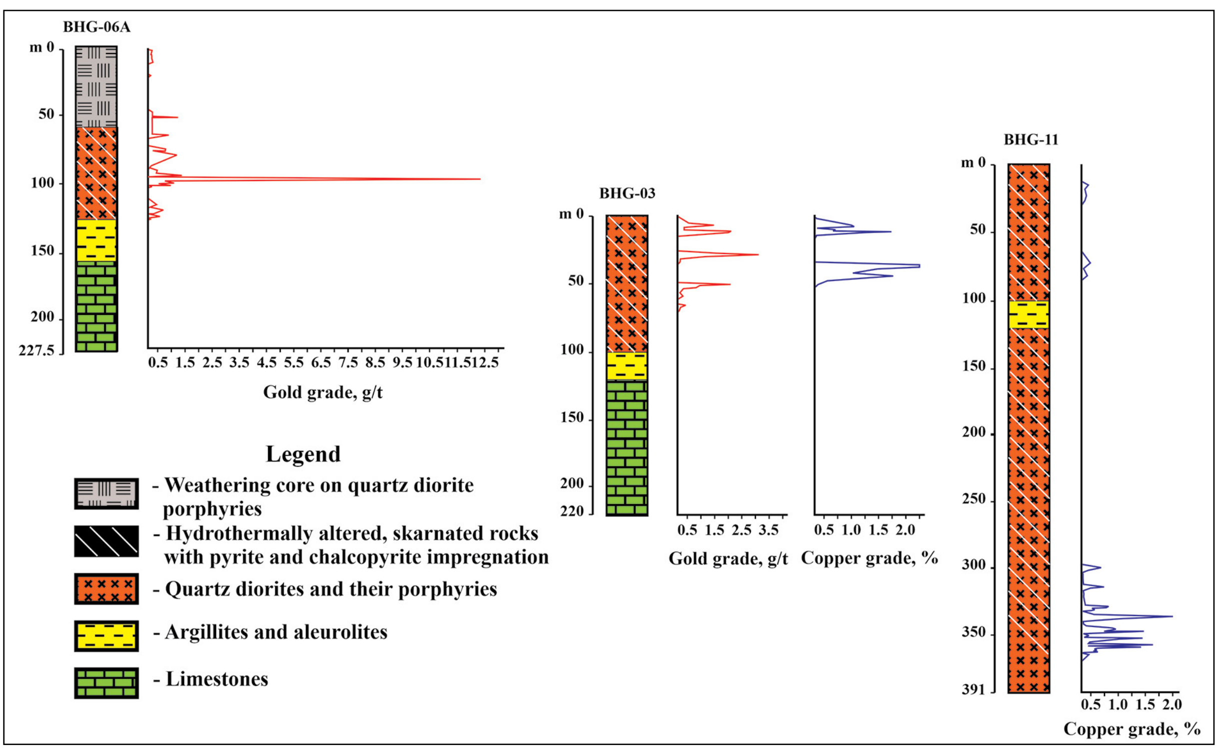

Figure 7- Vertical zoning of Gharta deposit.

the potential presence of high sulfidation gold ores. Thus, the district represents a promising target for exploration.

Figure 8 provides information on the geological structure of the mining district. The district was mapped by the author, alongside his postgraduate student, now Professor Archil G. Magalashvili, and subsequently detailed in my monograph (Tvalchrelidze, 2006). The central part of the mining district comprises the Merisi-Namonastrevi intrusive complex, covering an area of 17 km² and forming three outcrops: (i) Merisi outcrop with an area of 7.5 km², (ii) Namonastrevi outcrop (6.5 km²), and (iii) Chalati outcrop (2.5 km²). Detailed petrochemical investigations, along with fault mapping, have demonstrated that the Namonastrevi and Chalati outcrops were uplifted

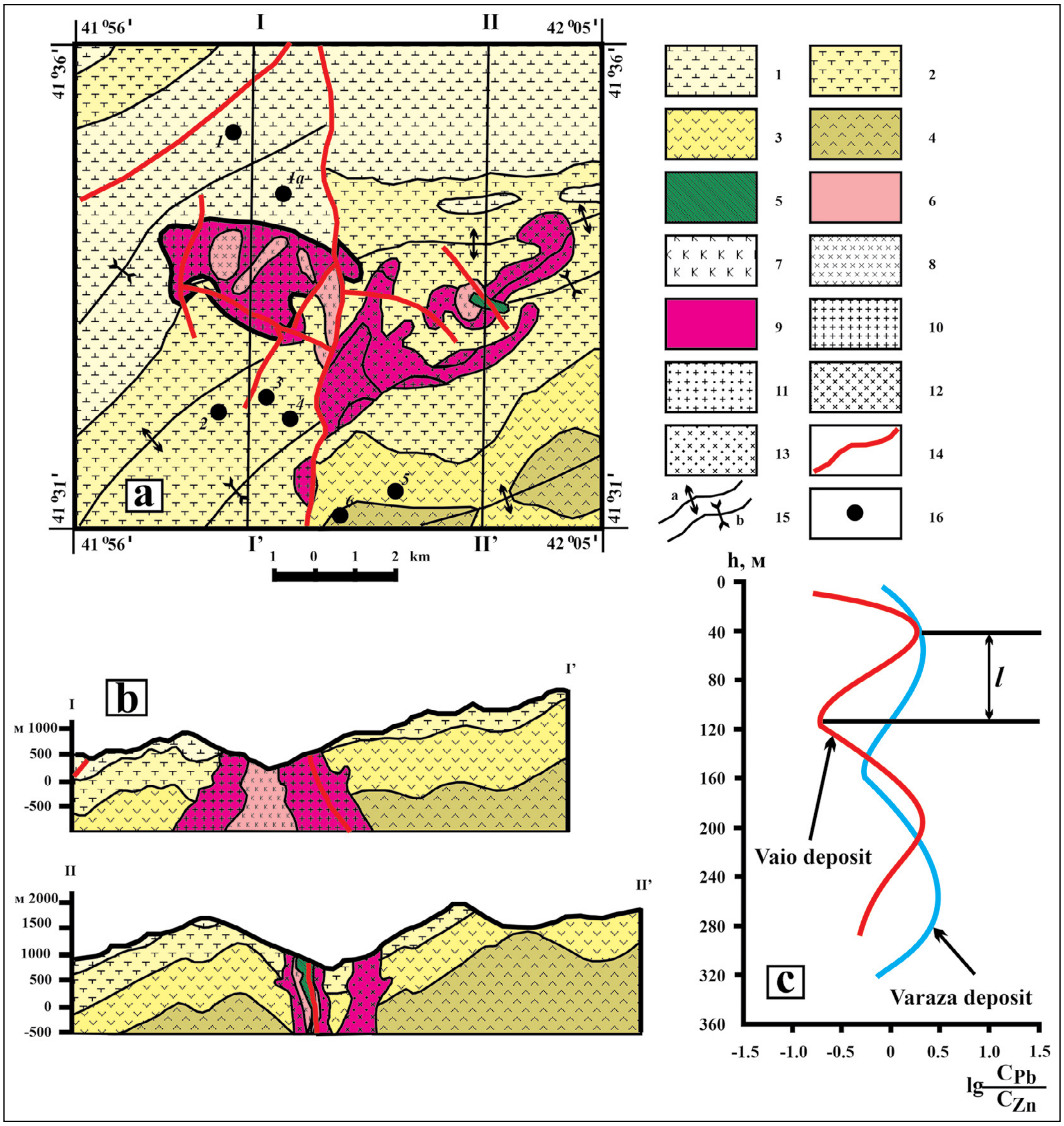

Figure 8- Geological structure of the Merisi mining district, a) geological map; b) cross sections to it. Legend: 1- Upper Eocene – Oligocene: trachybasalt lavas; 2- Upper Eocene: Calc-alkaline basalts and tuffs; 3- Middle Eocene: Subalkaline basalt-andesite-dacite volcanics; 4- Middle Eocene: Andesite tuffs; 5-13- intrusive rocks: 5- Fluid porphyry breccia phase, 6-8: quartz diorite porphyry phase: 6- subvolcanic bodies, 7- quartz diorite porphyries, 8- quartz diorites; 9-13: main intrusive phase: 9- the main intrusive complex, 10- alaskites, 11- granite porphyries, 12- monzonites, 13- diorite porphyries; 14- basic faults; 15- a) anticline and b) syncline axes; 16- intermediate sulfidation gold and base metal lodes: 1- Vaio, 1a- Surnali site of Vaio, 2- Veliburi, 3- Verkhnala, 4- Tskalbokela, 5- Varaza, 6- Obolo-Kanly-Kaia, c) vertical rhythmical zoning of lodes. l- pitch of rhythmicity, C_{Pb} and C_{Zn} – grades of lead and zinc, correspondingly.

along the sub-longitudinal fault by approximately 800 meters (Tvalchrelidze, 2006), causing out-cropping of differing acidic rocks in its western and eastern flanks. These investigations also revealed that the second quartz diorite porphyry phase intruded after the displacement along the mentioned fault had occurred, with rocks of this phase being consistent across each outcrop. The fluid porphyry breccia phase, in my opinion, marks the center of the porphyry ore-forming system and may serve as a significant exploration indicator.

All intermediate sulfidation gold and base metal epithermal deposits and occurrences within the district share a common structure. They are distanced from the contacts of the intrusive body, forming solely in country rocks as subvertical lodes of quartz ± barite composition, with varying thickness from a few meters up to 20 meters, but averaging 2-3 m. The matrix of these lodes bears impregnations and nests of sulfides, predominantly pyrite, chalcopyrite, galena, sphalerite, and also sulfosalts including sulfoantimonites, patrinite, clausthalite, etc. Near the surface, sulfides are oxidized to bornite, hematite, and others. Gold is present both in its native form as thin impregnations within the ores and as an admixture in iron, copper, lead, and zinc sulfides. The ore lodes are accompanied by thin, gouge-like halos of typical medium-temperature hydrothermal alteration, characterized by a quartz-sericite-chlorite rock. The ores are noted for their breccia texture.

The peculiarities of porphyry, high, and intermediate sulfidation systems, as described here, form a solid foundation for further discussion.

4. Discussion

Investigations into the thermodynamic conditions for the evolution of hydrothermal systems from a porphyry stage to the low sulfidation stage have been conducted by Einaudi et al., (2003). I performed a similar type of study sixteen years earlier (Tvalchrelidze, 1986; 1987). For instance, Figure 9 represents a thermodynamic plot demonstrating the equilibria between crystallizing minerals and a model hydrothermal fluid at a temperature of 250°C.

Analysis of this plot leads to the same main conclusion made by Einaudi et al. (2003): The

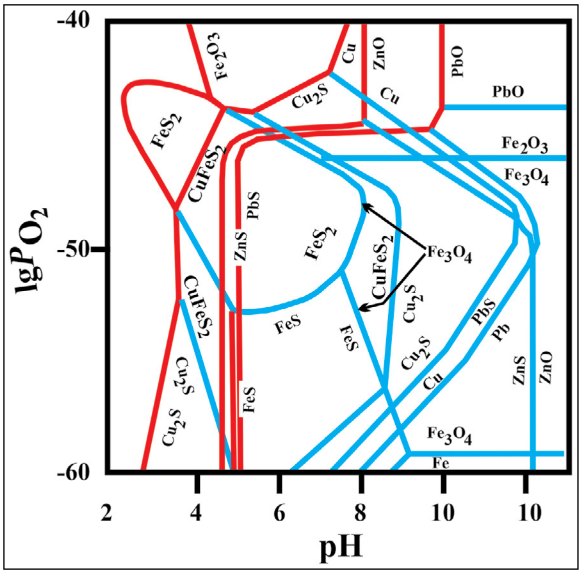

Figure 9- Equilibria of iron and base metal minerals with a model hydrothermal fluid at 250°C. Parameters of the model fluid were published earlier (Tvalchrelidze, 1987). Blue lines – equilibria between solid phases; red lines – equilibria between solid phases and a model fluid.

development of the system and gradual crystallization of minerals occur against the backdrop of fluid neutralization. However, this type of analysis does not explain the origination of convective fluid flows nor ore formation, e.g., mass precipitation of ore minerals within a comparatively limited time period and space. Moreover, the basic typomorphic features of epithermal systems are not addressed.

Some time ago, I analyzed data on an enormous number of vein deposits and demonstrated that practically all of them are characterized by a rhythmical zoning, meaning that the grade ratios of the main ore-forming metals undergo rhythmical fluctuations in the vertical section (Tvalchrelidze, 1993). Here, this phenomenon is demonstrated for two deposits of the Merisi mining district (Figure 8c). The pitch of such zoning, *l*, is proportional to the overall vertical interval of the lode. I further proved that this phenomenon is determined by ore formation in non-equilibrium conditions under the influence of a thermal gradient. In such an environment, metal cations tend to be bound by the sulfide ion, and different reactions of metal sulfides' precipitation compete with each other. Based on this simple assumption, I elaborated mathematical and thermodynamic models of such non-equilibrium reactions and formulated the theory of rhythmical zoning (Tvalchrelidze, 1993). This theory illustrated the distribution of bonanzas and vertical zoning of ore lodes but was unable to explain the formation of gold ores in high sulfidation epithermal deposits.

$$Zn^{2+} + S_2^{2-} \xrightarrow{k_1} ZnS$$
$$Pb^{2+} + S_2^{2-} \xrightarrow{k_2} PbS \qquad (1)$$

Correspondingly, kinetic coefficients k_1 and k_2 depend on the oversaturation degree of corresponding metals. Based on this simple assumption, it has been elaborated mathematical and thermodynamic models of such non-equilibrium reactions and formulated the theory of rhythmical zoning (Tvalchrelidze, 1993). This theory illustrated distribution of bonanza zones and vertical zoning of ore lodes but was unable to explain formation of gold ores in epithermal high sulfidation deposits.

Indeed, as shown in Figure 10, gold remains dissolved in a hydrothermal fluid under a wide range of P-T conditions. This phenomenon is suggested to be related to gold's dual position within the common acid-alkali range of metals. Firstly, gold is encountered together with iron in slightly acidic fluids. Secondly, it is deposited from low-temperature fluids at the final stages of ore formation (Kolonin, 1983). This peculiarity can be explained by the well-expressed chemical affinity of gold with arsenic (Marakushev and Bezmen, 1970), which, in a high-temperature fluid, is presented in the form of the acid at the line of monovariant equilibrium between hydrogen sulfide and sulfuric acid (Figure 10). However, in a low-temperature fluid, arsenic assumes the role of metal. Consequently, gold plays no role in competitive sulfide deposition processes, gradually precipitates from a fluid with a fall in temperature, creating concentrations far below the cutoff grade, and in normal evolution of high sulfidation hydrothermal systems, is unable to form mineral deposits.

Thus, the sole reason for gold precipitation when a high and/or intermediate sulfidation epithermal mineralization forms is a sharp disruption of the consecutive ore formation process due to external influences. One such influence is the phreatic collapse of the ore-hosting structures, followed by the boiling of the hydrothermal fluid and mass precipitation of its ore content.

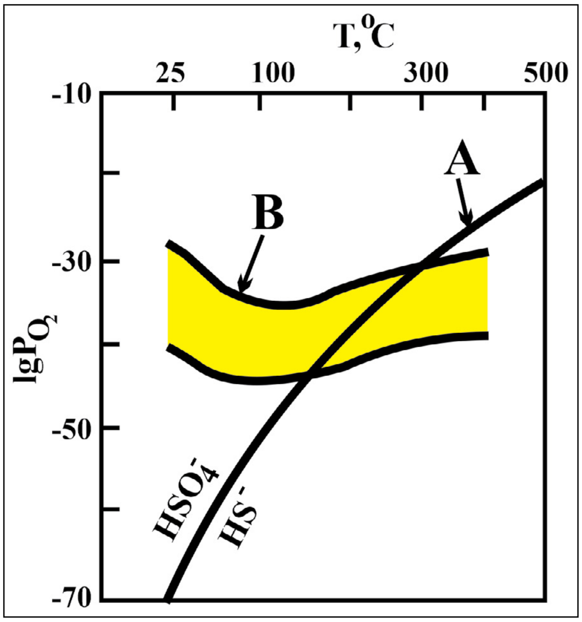

Figure 10- Partial pressure of oxygen during crystallization of base metal sulfides and barite. After Tvalchrelidze (2006), A – monovariant equilibrium Line between S^{6+} and S^{2-} B – field of gold stability in a hydrothermal fluid.

1. The presence of hydrothermal breccias, often with jigsaw-fit texture, specifically highlighted in our studies (Figure 4a), or vuggy silica (Figure 6a), is evidence of such a collapse. This indicates that hydrothermal breccia has a phreatic origin. It should be noted that phreatic breccias are often described in models of high and/or intermediate sulfidation systems. However, several features characteristic of either porphyry or epithermal systems do not align with a purely thermodynamic approach. Specifically: Intermediate and low sulfidation mineralizations are typically located at a certain distance from the contacts of the intrusive body. My earlier statistical analysis of numerous plutonogenic ore districts demonstrated that this distance directly correlates with the dimensions of the plutonic body.

2. A direct transition between porphyry and high sulfidation ores is never observed. In every case I have studied, a distinct ore-free space exists between the two, even though this interval undergoes the same hydrothermal alteration as the ore-rich zones.

3. Porphyry copper ores are often hosted by the main intrusive body, suggesting that they formed simultaneously with or shortly after the crystallization

of the host rock. This observation challenges models that rely solely on a peripheral magmatic source for mineralization.

Given these insights, the significance of employing paleothermophysical models to examine the cooling of intrusive bodies becomes evident. Among the early pioneers of such research was my colleague from Moscow State University, Doctor of Geology and Mineralogy, Vladimir G. Zolotarev. Tragically, Zolotarev and his family met a fatal end in a car accident in the early nineties of the recent century. Honoring his memory and building upon his foundational work, I have continued these investigations and developed a model specifically for the Merisi mining district. This endeavor not only serves as a tribute to Zolotarev's contributions to geology but also advances our understanding of the thermal dynamics and mineralization processes within intrusive geological formations.

Dr. Zolotarev's methodology is predicated on fundamental principles (Zolotarev, 1985): Upon intrusion, the temperature of the magmatic fusion significantly surpasses that of the surrounding country rocks. Consequently, in accordance with the Second Law of thermodynamics, an immediate heat exchange begins between the magma and the host rocks—resulting in the cooling and crystallization of the magma, while simultaneously heating the country rocks. The modeling of such thermal fields necessitates the application of the classical Fourier equation of heat and mass transfer, which encapsulates both convective and conductive heat and mass flows (2). This approach allows for a nuanced understanding of the thermal interactions within geological systems, providing a comprehensive framework for analyzing the cooling patterns of magmatic bodies and their consequent effects on the surrounding geological environment.

$$C\rho(\frac{\partial T}{\partial t}) = -\nabla(q_L h_L + q_S h_S) + \nabla(\lambda \nabla T) + F', \quad (2)$$

Where: ρ = density, C = heat conductivity, T = temperature, t = time, λ = heat conductivity factor, h_L and h_S = enthalpy of fusion's liquid and gaseous phases, q_L and q_S = fusion and liquid phases masses, passing through the elementary 1 cm^2 section, F' = latent fusion heat determining phase change, ∇ = Hamilton's operator. In 3D Descartes space the latter may be expressed as:

$$\nabla = (\frac{\partial}{\partial X} + \frac{\partial}{\partial Y} + \frac{\partial}{\partial Z}), \quad (3)$$

Zolatarev (1985) has proven that in thermophysical models of a cooling magmatic body the influence of the convective member of the Fourier's equation is negligible. In this case, development of the heat field through time may be described by the classical equation of heat transfer:

$$C\rho(\frac{\partial T}{\partial t}) = div(\lambda gradT) + F'(x, y, z), \quad (4)$$

It can be straightforwardly demonstrated that equation (4) is exponential in nature and lacks an analytical solution. Consequently, the modeling of heat fields ought to be conducted in accordance with the methodology proposed by Zolotaev (1985 and subsequent works). This process involves segmenting the entire geological space into a requisite number of elementary blocks, each characterized by a uniform composition and precise coordinates within Cartesian space. Subsequently, the heat transfer equation is to be resolved individually for each of these elementary blocks, ensuring a detailed and accurate representation of the thermal dynamics within the geological setting. This granular approach allows for a comprehensive analysis of heat distribution and its effects on mineralization processes across the spatial extent of the geological environment under study.

$$C\rho(\frac{\partial T}{\partial t}) = \lambda(\frac{\partial^2 T}{\partial t^2}) + F', \quad (5)$$

And for each time interval Δt heat amount (ΔQ) may be calculated for each block having coordinates *i*, *j*, *k*, and the block will have temperature:

$$T'_{i,j,k} = T_{i,j,k} + \Delta T; \Delta T = \frac{\Delta Q}{C_V}, \quad (6)$$

Where: $T_{i,j,k}$ = is a temperature in time moment *t*, whereas $T'_{i,j,k}$ = is temperature in time moment $t + \Delta t$, C_V = specific heat conductivity of the given block. As far as this method is based on successive temperature calculation along coordinate axes, the stability condition must be respected: Time pitch shall be followed by a pitch along axes:

$$\partial t \leq (\frac{1}{2}k)(\frac{\lambda_{\max}}{C.l})l_0; k = 1,2, \quad (7)$$

Where: l_0 = distance between blocks. In 2D models this condition may be satisfied by calculation of heat transfer between blocks:

$$C\rho(\frac{\partial T}{\partial t} + V\Delta T) = div(\lambda gradT) + F', \quad (8)$$

Where: $\vec{V}$ = speed vector of heat transfer.

I have developed a specific model for the Merisi mining district. The thermophysical parameters crucial for these calculations were previously documented (Tvalchrelidze, 2006). Figure 11 illustrates a block model of the geological environment at a depth of 2.5 kilometers, captured before the occurrence of fault tectonics events and the intrusion of the second phase. Figure 12 elucidates the dynamics of crystallization and paleotemperature fields 122,000 years following the intrusion. Indeed, paleotemperature fields underwent analysis across various temporal spans, specifically: 6, 14, 22, 30, 46, 80, 122, 160, 180, and 250 thousand years post-intrusion. Nevertheless, the epoch 122,000 years subsequent to the intrusion is of paramount significance, as by this juncture, the massif had fully crystallized (as depicted in Figure 12a). This complete crystallization precipitated a phase of paleothermal field stabilization extending from, at a minimum, 122,000 to 250,000 years after the intrusion.

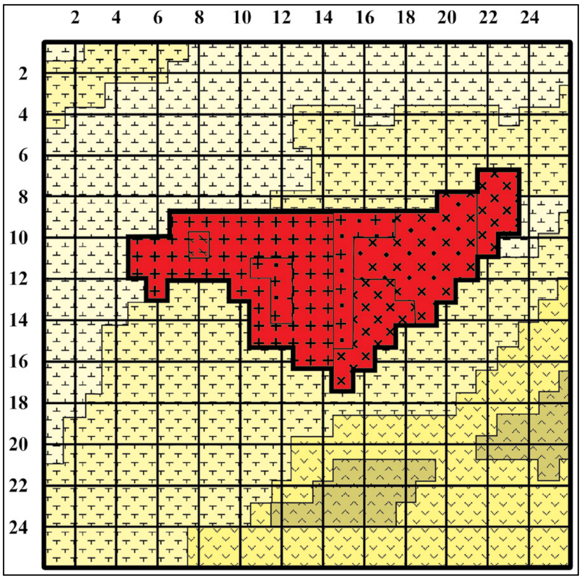

Figure 11- Block model of the Merisi geological environment at a depth of 2.5 km immediately after intrusion of the main phase. Block numbers along coordinate axes are shown. Legend see on Figure 8.

The data presented herein enable the articulation of several foundational postulates, which are discussed in the subsequent sections.

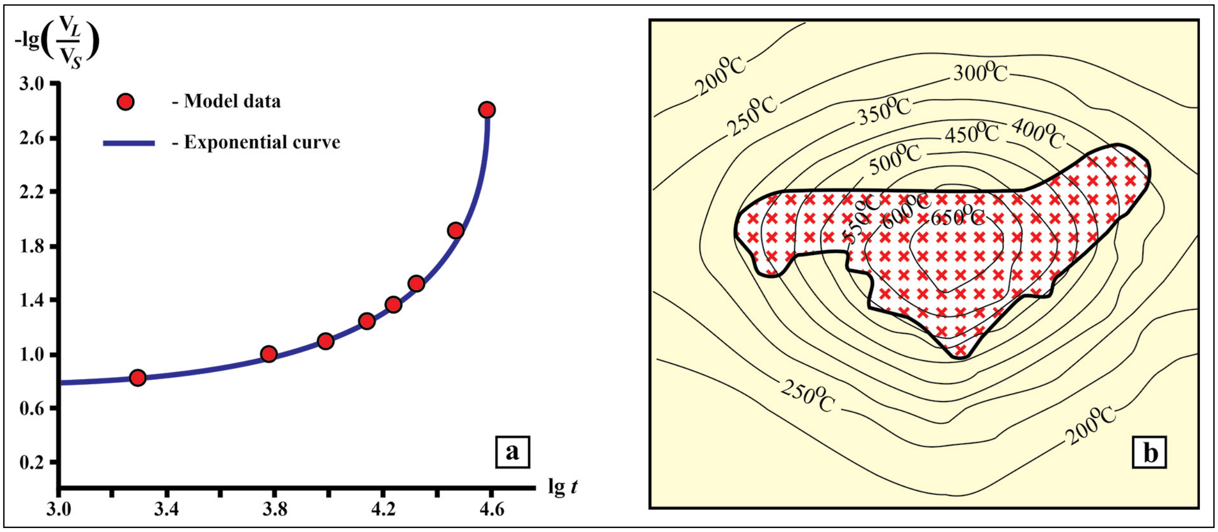

Figure 12- Succession of crystallization, a) and paleotemperature field 122,000 years after intrusion, b) of the Merisi Pluton. V_L and V_S = correspondingly, volumes of the fusion and the crystalized phases; t = time in years.

5. Results

The classical thermodynamic model, which interprets the formation of sulfide minerals as reactions of mineral precipitation under equilibrium conditions, fails to account for the genesis of conventional flows of meteoric waters or the formation of ores of the type under investigation. In the context of porphyry and epithermal ore formation, several prerequisite conditions are proposed to be essential:

1. Source of anomalous energy (heat), which exceeds normal thermodynamics of the enclosing environment.

2. The presence of temperature (and heat!) gradient, which determines conventional flows of fluids composed of endogenous and meteoric constituents (proven by rhythmical zoning of ore lodes).

3. The persistence of such conditions for a period of sulfide ore formation – shorter this stability period is, smaller deposit is formed.

These conditions can be generated through various geological processes, including the transfer of heat from a peripheral magmatic source, a mechanism commonly incorporated into models of epithermal deposit formation. Nevertheless, these models fall short in addressing scenarios involving complex ore-forming systems where porphyry and high and/or intermediate sulfidation ores coexist. In such instances, the requisite heat for ore formation emanates from the paleothermal field associated with cooling magmatic complexes. This specific environment establishes a number of fundamental characteristics inherent to these amalgamated systems, as outlined below:

1. In expansive porphyry copper (± gold) deposits, the porphyry ores are predominantly situated near the contacts (both endo- and exocontacts) of the intrusive massifs. In contrast, within smaller deposits, these ores may be found in the central regions of the igneous body. This distribution pattern becomes intelligible when considering the paleothermal history of the cooling intrusive massifs. As evidenced by Figure 12b, at the juncture when thermal fields reached stability, the temperature within the central part of the large massif remained excessively high for the deposition of ores.

2. This same thermal dynamic also explains the lack of direct telescoping from porphyry ores into high sulfidation mineralization. It has been observed that an interval of ore-free zones exists between these two types of mineralization, corresponding to a reduction in temperature to levels conducive for the formation of epithermal ores.

3. As the cooling magmatic body dissipates heat, it warms the surrounding country rocks. Over time, while the paleotemperature gradient tends to even out, the extent of the heated region expands. Consequently, a distinct gap is present between the initial intermediate sulfidation deposit and the intrusive body's contact. My previous statistical analyses of several plutonogenic ore districts (Tvalchrelidze, 2006) have demonstrated that the size of this gap is proportionate to the dimensions of the magmatic body, with a notably strong correlation. This finding underscores the significant influence of the thermal and structural characteristics of magmatic bodies on the spatial distribution of mineral deposits.

Therefore, the process of sulfide ore formation as outlined cannot account for the genesis of high sulfidation gold deposits. As elucidated, the widespread precipitation of free gold necessitates a phreatic collapse within the ore conduit channel subsequent to the formation of hydrothermally altered rocks. This catastrophic event leads to the formation of hydrothermal breccias, frequently characterized by a jigsaw-fit texture, or brecciated vuggy silica. In these formations, both the host rocks and the hydrothermally altered rocks are bound together by a gold-bearing quartz matrix. This phenomenon underscores the complexity of geological processes involved in high sulfidation gold deposit formation, highlighting the importance of dynamic geological events in the concentration of precious metals.

The model outlined in this article has been validated by the geological characteristics of the deposits discussed herein. This model has facilitated the development of a comprehensive exploration strategy and methodology, resulting in the discovery of multiple porphyry copper and high sulfidation epithermal gold deposits. Currently, four of these deposits are being extensively mined, and construction is underway at mines on two additional sites. Our team has successfully conducted explorations at several deposits, demonstrating the efficacy of our approach in identifying and developing valuable mineral resources. This success underscores the practical applicability of the model in guiding effective exploration efforts and enhancing the potential for discovering significant mineral deposits.

Acknowledgements

It is my pleasure to acknowledge the international team of economic geologists with whom I am successfully working and performing research for decades, and namely Dr Zurab Kutelia, Dr Revaz Kvatashidze, and Dr Irakli Narozauli (Georgia); Dr. Dmitry Pertel and Dr Paul Hanzl (Australia); Dr. Andrei Kharlashin (Russia), and many others.

It is my sad duty to remember my late colleagues the friendships and collaboration with whom passed through my entire professional life, and namely: Prof. Dr Veniamin Gogishvili, Dr Tina Gogishvili (Georgia); Prof. Dr Bogdan Bogdanov (Bulgaria); Prof. Dr Mirko Vaněček, Prof. Dr Zdenek Pouba (Czech Republic); Prof. Dr Valentin Naumenko, Dr Yuri Koptyukh (Ukraine); Dr Emin Suleymanov, Prof. Dr Vagif Ramazanov (Azerbaijan Republic); Dr Vladimir G. Zolotarev (Russia).

References

Adamia, S. A., Chkhotua, T., Kekelia, M., Lordkipanidze, M., Zakariadze, G. 1981. Tectonics of the Caucasus and adjoining regions: implications for the evolution of the Tethys ocean. Journal of Structural Geology, 3, 437-447.

Adamia, S., Zakariadze, G., Chkhotua, T., Sadradze, N., Tsereteli, N., Chabukiani, A., Gventsadze, A. 2011. Geology of the Caucasus: A review. Turkish Journal of Earth Sciences, 20 (5), 489-544.

Aghazadeh, M., Hou, Z., Badrzadeh, Z., Zhou, L. 2015. Temporal-spatial distribution and tectonic setting of porphyry copper deposits in Iran: Constraints from zircon U-Pb and molybdenite Re-Os geochronology. Ore Geology Reviews, 70 (4), 385-406.

Aluç, A., Kuşcu, I., Peytcheva, I., Cihan, M., von Quadt, A. 2020. The late Miocene Öksüt high sulfidation epithermal Au-Cu deposit, Central Anatolia, Türkiye: Geology, geochronology, and geochemistry. Ore Geology Reviews, 126, 103795.

Arribas Jr., A. 1995. Characteristics of high sulfidation epithermal deposits, and their relation to magmatic fluid. Thompson, J.F.H. (ed.) Magmas, Fluids, and Ore Deposits. Mineralogical Association of Canada Short Course, 23, 419-454.

Berberian, M., King, G. C. P. 1981. Toward a paleogeography and tectonic evolution of Iran. Canadian Journal of Earth Science, 18, 210–265.

Berger, B. R., Ayuso, R. A., Wynn, J. C., Seal, R. R. 2008. Preliminary model of porphyry copper deposits. Open-File Report 2008-1321. U.S. Department of the Interior, U.S. Geological Survey. Reston, 62.

Bogdanov, K., Musaev, S., Ahmedov, A., Salmanli, R. 2013. High-sulphidation (HS) epithermal gold mineralisation in the Chovdar deposit, Lesser Caucasus, Azerbaijan. Proceedings of Bulgarian Geological Society National Conference with international participation "GEOSCIENCES 2013". Sofia, 15-16.

Boomeri, M., Nakashima, K., Lentz, D. R. 2010. The Sarcheshmeh porphyry copper deposit, Kerman, Iran: A mineralogical analysis of the igneous rocks and alteration zones including halogen element systematics related to Cu mineralization processes. Ore Geology Reviews, 38 (4), 367-381.

Cas, R., Giordano, G., Balsamo, F., Esposito, A., Lo Mastro, S. 2011. Hydrothermal Breccia Textures and Processes: Lisca Bianca Islet, Panarea Volcano, Aeolian Islands, Italy. Economic Geology, 106, 437-450.

Diarra, K., Sangu, E., Çiftçi. E. 2019. Ore mineralogy of high sulfidation Çorak-Taç epimesothermal gold deposit (Yusufeli-Artvin-Türkiye). Glagolev, S. (ed.) Proceedings of 14th International Congress for Applied Mineralogy (ICAM2019), Springer Nature Switzerland AG. Cham, 53–58.

Einaudi, M. T., Hedenquist, J., Inan, E. E. 2003. Sulfidation state of fluids in active and extinct hydrothermal systems: Transitions from porphyry to epithermal environments. Volcanic, Geothermal and Ore-Forming Fluids: Rulers and Witnesses of Processes within the Earth. Special Publication 10. Society of Economic Geologists. Ottawa, 285-311.

Engin, T. 2003. Mineral Deposits of Türkiye. Tvalchrelidze, A.G., Morizot, G. (eds). Mineral Resource Base of the Southern Caucasus and Systems for its Management in XXI Century. Kluwer Academic Publishers. Dordrecht-Boston-London, 81-104.

Ersoy, A. 2022. The current status of gold mining in Türkiye: An overview. NOHU Journal of Engineering Sciences, 11(4), 1103-1114.

Ghaderi, M., Narges, Y., Mina, B. K. 2018. Porphyry copper deposits of Iran. Tarbiat Modarres University Press. Tehran, 668.

Goldfarb, R. J., Groves, D. I., Gardoll, S. 2001. Orogenic gold and geologic time: a global synthesis. Ore Geology Reviews, 18 (1-2), 1-75.

Gülyüz, N., Gülyüz, E., Shipton, Z. K., Kuşcu, İ., Lord, L. A. 2020. Geological and mineralization characteristics of the Kestanelik epithermal Au-Ag deposit in the Tethyan Metallogenic Belt, NW Türkiye. Geoscience Journal, 24, 407–424.

Hajalilou, B., Aghazadeh, M. 2016. Geological, alteration and mineralization characteristics of Ali Javad Porphyry Cu-Au deposit, Arasbaran Zone, NW Iran. Open Journal of Geology, 6, 859-874.

Hastorun, S. 2022. The mineral industry of Türkiye. 2019 Minerals Yearbook. Türkiye. U.S. Department of the Interior, U.S. Geological Survey. Manto Park, 47.1-47.19.

Hedenquist, J. W. 2000. Exploration for epithermal gold deposits. SEG Reviews, 13, 245-277.

Heidari, S. M., Daliran, F., Paquette, J. -L., Gasquet, D. 2015. Geology, timing, and genesis of the high sulfidation Au (-Cu) deposit of Touzlar, NW Iran. Ore Geology Reviews, 65, 460–486.

Hosseini, S. A., Asghari, O., Emery, X. 2017. Direct block-support simulation of grades in multi-element deposits: application to recoverable mineral resource estimation at Sungun porphyry copper-molybdenum deposit. The Journal of the South African Institute of Mining and Metallurgy, 117, 577-585.

Imamverdiyev, N. A., Baba-zadeh, V. M., Mursalov, S. S., Valiyev, A. A., Mansurov, M. I., Abdullayeva, S. F. 2021. New perspective Reza gold deposit (Gedabek ore district, Lesser Caucasus, Azerbaijan). Journal of Geology, Geography and Geoecology. 30 (1), 53-64.

John, D.A. (Ed.). 2010. Porphyry copper deposit model. Scientific Investigations Report 2010-5070-B. U.S. Department of the Interior, U.S. Geological Survey, Reston, 170.

John, D. A., Vikre, P. G., du Bray, E. A, Blakely, R. J., Fey, D. L., Rockwell, B. W., Mauk, J. L., Anderson, E. D., Graybeal, F. T. 2018. Descriptive models for epithermal gold-silver deposits. Mineral Deposit Models for Resource Assessment. Scientific Investigations Report 2010–5070–Q. U.S. Department of the Interior, U.S. Geological Survey. Reston, 264.

Kaviani, A., Hatzfeld, D., Paul, A., Tatar, M., Priestley. K. 2009. Shear-wave splitting, lithospheric anisotropy, and mantle deformation beneath the Arabia-Eurasia collision zone in Iran. Earth and Planetary Science Letters, 286 (3-4), 371–378.

Kolonin, G. R. 1983. Acidity and alkalinity evolution character in ore-forming fluid based on experimental data. Dobretsov, N.L. (ed.) Dynamic and Physical-Chemical Models of Magmatic Systems.: Nauka Publisher. Novosibirsk, 57-70 (in Russian).

Kuşcu I., Tosdal, Richard M., Gençalioğlu-Kuşcu, G. 2019. Chapter 8. Porphyry-Cu Deposits of Türkiye. Pirajno, F., Ünlü, T., Dönmez, C., Şahin, B.M. (eds): Mineral Resources of Türkiye. Springer Nature Switzerland AG. Cham, 337-425.

Marakushev, A. A., Bezmen, N.I. 1970. Thermodynamics of sulfides and oxides related to ore formation problems. Nauka Publisher. Moscow, 215 (in Russian).

Marutani, M. 2003. Study on mining sector development master plan in the Republic of Armenia. Final report. Japan International Cooperation Agency (JICA), Steering Committee of Study on Mining Sector Development Master Plan of Government of the Republic of Armenia. Yerevan-Tokyo, 46.

Mederer, J., Moritz, R., Ulianov, A., Chiaradia. M. 2013. Middle Jurassic to Cenozoic evolution of arc magmatism during Neotethys subduction and arc-continent collision in the Kapan Zone, southern Armenia. Lithos, 177, 61-78.

Mehrabi, B., Chaghaneh, N., Fazel, E. T. 2008. Intermediate sulfidation epithermal mineralization of No. 4 anomaly of Golojeh deposit (N. Zanjan) based on mineralography, alteration and ore fluid geochemistry features. Journal of Economic Geology, 6 (1), 1-22.

Mehrabi, B., Sianib, M. G., Azizic, H. 2014. The genesis of the epithermal gold mineralization at North Glojeh Veins, NW Iran. International Journal of Sciences: Basic and Applied Research (IJSBAR), 15 (1), 479-497.

Moritz, R., Rezeau, H., Ovtcharova, M., Tayan, R., Melkonyan, R., Hovakimyan, S., Ramazanov, V., Selby, D., Ulianov, A., Chiaradia, M., Putlitz, B. 2016. Long-lived, stationary magmatism and pulsed porphyry systems during Tethyan subduction to post-collision evolution in the southernmost Lesser Caucasus, Armenia and Nakhitchevan. Gondwana Research, 37, 465-503.

Moritz, R., Reseau, H., Mederer, J., Gialli, S., Hemon, P., Lavoie, J., Calder, M., Hovakimyan, S., Melkonyan,, R., Tayan, R., Popkhadze, N., GuGushvili, V., Ramazanov, V. 2017. Gold deposits of the Lesser Caucasus: products of successive Mesozoic and Cenozoic geodynamic settings. Mineral Resources to Discover – Proceedings of the 14th SGA Biennial Meeting, 1. Society for Geology Applied to Mineral Deposits. Geneve, 67-70.

Oyman, T., Minareci, F., Pişkin, Ö. 2003. Efemçukuru B-rich epithermal gold deposit (İzmir, Türkiye). Ore Geology Reviews, 23, (1-2), 35-53.

Payot, B. D., Maglambayan, V. B., Dimalanta, C. B., Yumul Jr., G. P., Tamayo Jr., R. A., Matsuda, T., Suzuki, S., Bellon, H. 2005. Geology and hydrothermal alteration of the low sulfidation Pantingan Gold System, Mount Mariveles, Bataan (Luzon), Philippines. Resource Geology, 55 (3), 155-162.

Richards, J. P. 2015. Tectonic, magmatic, and metallogenic evolution of the Tethyan orogen: From subduction to collision. Ore Geology Reviews, 70, 323-345.

Shafiei, B., Shahabpour, J. 2008. Gold distribution in porphyry copper deposits of Kerman Region, southeastern Iran. Journal of Sciences, 19 (3), 247-260.

Sholeh, A., Rastad, E., Huston, D., Gemmell, J.B., Taylor, R.D. 2016. The Chahnaly low-sulfidation epithermal gold deposit, Western Makran volcanic arc, southeast Iran. Economic Geology, 111, 619–639.

Sillitoe, R. H. 2000. Styles of high-sulphidation gold, silver and copper mineralisation in porphyry and epithermal environments. Proceedings of the Australasian Institute of Mining and Metallurgy, 305, 19-34.

Sinclair, W. D. 2007. Porphyry Deposits. Goodfellow, W.D. (ed.) Mineral Deposits of Canada: A Synthesis of Major Deposit-Types, District Metallogeny, the Evolution of Geological Provinces, and Exploration Methods. Geological Association of Canada, Mineral Deposits Division, Special Publication No. 5, 223-243.

Taylor, B. E. 2007. Epithermal gold deposits. Goodfellow, W.D. (ed.) Mineral Deposits of Canada: A Synthesis of Major Deposit-Types, District Metallogeny, the Evolution of Geological Provinces, and Exploration Methods. Geological Association of Canada, Mineral Deposits Division, Special Publication No. 5, 113-139.

Tvalchrelidze, A. G. 1980. Copper metallogeny of the Caucasus. Jankovic, S. (ed.) European Copper Deposits. Belgrade, 191-196.

Tvalchrelidze, A. G. 1984. Main features of metallogeny of the Caucasus, Janelidze, T.V., Tvalchrelidze, A.G. (eds): Proceedings of the Sixth Quadrennial IAGOD Symposium. Vol. 1. E. Schweizerbat'sche Verlagbuchhandlung. Stuttgart, 1-5.

Tvalchrelidze, A. G. 1986. Physico-chemical conditions of base metal sulphide ore formation. Friedrich, G. H., Genkin, A. D., Naldrett, A. J. Ridge, J. D., Sillitoe, R. H. Vokes, F. M. (eds.) Geology and Metallogeny of Copper Deposits. Springer-Verlag. Berlin-Heidelberg-New York-London-Paris-Tokyo, 358-369.

Tvalchrelidze, A. G. 1987. Geochemical conditions of base metal sulfide deposit formation. Nedra Press. Moscow, 188 (in Russian).

Tvalchrelidze, A. G. 1993. Quantitative models of vein type ore deposits and theory of rhythmical zoning. Geological Association of Canada Special Papers, 40, 751-760.

Tvalchrelidze, A. G. 2003. Mineral resource base of Georgia in XXI century. Tvalchrelidze, A.G., Morizot, G. (eds.) Mineral Resource Base of the Southern Caucasus and Systems for its Management in the XXI Century. Kluwer Academic Publisher. Dordrecht-Boston-London, 19-70.

Tvalchrelidze, A. G. 2006. Mineral resources and mineral resource base of Georgia. Rudy I Metally Publishing House. Moscow, 320 (in Russian).

Veliyev, A., Bayramov, A., Ibrahimov, J., Mammadov, S., Alizhadeh, G. 2018. Geological setting and ore perspective of the new discovered Gadir low sulfidation epithermal deposit, Gedabek NW flank, Lesser Caucasus, Azerbaijan. Universal Journal of Geoscience, 6 (3), 78-101.

Wang, L., Qin, K., Song, G., Li, G. 2019. A review of intermediate sulfidation epithermal deposits and subclassification. Ore Geology Reviews 107, 434-456.

Yiğit, O. 2006. Gold in Türkiye – a missing link in Tethyan metallogeny. Ore Geology Reviews, 28 (2), 147-179.

Yiğit, O. 2009. Mineral deposits of Türkiye in relation to Tethyan metallogeny: Implications for future mineral exploration. Economic Geology, 104 (1), 19-51.

Zolotarev, V. G. 1985. Spatial-temporal dynamics of processes related to granite consolidations and their role in ore formation. Sciences de Terre. Série Information géologique, 23, 27-48.